Radiation Physics and Chemistry 137 (2017) 187–192

Contents lists available at ScienceDirect

Radiation Physics and Chemistry

journal homepage: www.elsevier.com/locate/radphyschem

The HEPD particle detector and the EFD electric field detector for the CSES satellite

L. Alfonsi[n], F. Ambroglini[i], G. Ambrosi[g], R. Ammendola[b], D. Assante[l,b], D. Badoni[b], V.A. Belyaev[q], W.J. Burger[o,c], A. Cafagna[k,c,p], P. Cipollone[b], G. Consolini[m], L. Conti[l,b,*], A. Contin[h,d], E.De Angelis[m], C.De Donato[b], G.De Franceschi[n], A.De Santis[n], C.De Santis[b], P. Diego[m], M. Durante[c], C. Fornaro[l,b], C. Guandalini[d], G. Laurenti[h,d], M. Laurenza[m], I. Lazzizzera[k], M. Lolli[d], C. Manea[c], L. Marcelli[b,j], F. Marcucci[m], G. Masciantonio[b], G. Osteria[f], F. Palma[b,j], F. Palmonari[d,h], B. Panico[f], L. Patrizii[d], P. Picozza[j,b,l], M. Pozzato[d], I. Rashevskaya[c], M. Ricci[e], M. Rovituso[c], V. Scotti[f], A. Sotgiu[b], R. Sparvoli[j,b], B. Spataro[e], L. Spogli[n], F. Tommasino[c], P. Ubertini[m], G. Vannaroni[l,m], S. Xuhui[p], S. Zoffoli[a], The CSES-LIMADOU Collaboration

[a] *Agenzia Spaziale Italiana, V. del Politecnico snc, 00133 Rome, Italy*
[b] *INFN - Sezione Roma 2, V. della Ricerca Scientifica 1, 00133, Rome, Italy*
[c] *INFN - TIFPA, V. Sommarive 14, 38123 Povo TN, Italy*
[d] *INFN Sezione of Bologna, V.le Berti Pichat 6/2, Bologna, Italy*
[e] *INFN - LNF, V. E. Fermi, 40, 00044 Frascati RM, Italy*
[f] *INFN Sezione of Napoli, via Cintia, I-80126, Napoli, Italy*
[g] *INFN Sezione of Perugia, V. A. Pascoli, 06123, Perugia, Italy*
[h] *University of Bologna, V.le Berti Pichat 6/2, Bologna, Italy*
[i] *University of Perugia, V. A. Pascoli, 06123, Perugia, Italy*
[j] *University of Tor Vergata, V. della Ricerca Scientifica 1, 00133 Rome, Italy*
[k] *University of Trento, V. Sommarive 14, 38123 Povo TN, Italy*
[l] *Uninettuno University, C.so V. Emanuele II, 39, 00186, Rome, Italy*
[m] *INAF-IAPS, V. Fosso del Cavaliere 100, 00133, Rome, Italy*
[n] *INGV, V. di Vigna Murata 605, 00143 Rome, Italy*
[o] *Fondazione Bruno Kessler, I-38122 Trento, Italy*
[p] *CEA, #1 An Ningzhuang Road, 100085 Haidian District, Beijing, China*
[q] *National Research Nuclear University MEPhI, Moscow, Russia*

ARTICLE INFO

Keywords:
Particle detector
Electric field detector
Magnetosphere
Ionosphere
Space Weather
Cosmic rays
Earthquake
Seismic-precursors

ABSTRACT

The CSES satellite, developed by Chinese (CNSA) and Italian (ASI) space Agencies, will investigate iono-magnetospheric disturbances (induced by seismicity and electromagnetic emissions of tropospheric and anthropogenic origin); will monitor the temporal stability of the inner Van Allen radiation belts and will study the solar-terrestrial coupling by measuring fluxes of cosmic rays and solar energetic particles. In particular the mission aims at confirming the existences (claimed from several analyses) of a temporal correlations between the occurrence of earthquakes and the observation in space of electromagnetic disturbances, plasma fluctiations and anomalous fluxes of high-energy particles precipitating from the inner Van Allen belt. CSES will be launched in the summer of 2017 with a multi-instruments payload able to measure: e.m. fields, charged particles, plasma, TEC, etc. The Italian LIMADOU collaboration will provide the High-Energy Particle Detector (HEPD), designed for detecting electrons (3–200 MeV) and proton (30–300 MeV)), and participates to develop the Electric Field Detector (EFD) conceived for measuring electric field from ~DC up to 5 MHz.

* Corresponding author at: University of Trento, V. Sommarive 14, 38123 Povo, TN, Italy.
E-mail address: livio.conti@uninettunouniversity.net (L. Conti).

http://dx.doi.org/10.1016/j.radphyschem.2016.12.022
Received 3 November 2015; Received in revised form 23 November 2016; Accepted 28 December 2016
Available online 30 December 2016
0969-806X/

1. Introduction

CSES (China Seismo-Electromagnetic Satellite) is a satellite mission devoted to monitor the near-Earth electromagnetic, plasma and particle environment (Xuhui, 2011). The main objectives of the mission are: (i) to study possible coupling mechanisms between lithosphere, atmosphere, ionosphere and magnetosphere and (ii) to study the solar-terrestrial interactions and cosmic rays in the range from few MeV up to hundreds of MeV. The instruments on board the satellite have been conceived and built in order to investigate electromagnetic field as well as plasma and particles perturbations of the atmosphere and ionomagnetosphere induced by natural sources, anthropocentric emitters and seismic events.

In occasion of many earthquakes of medium and high magnitude and volcanic eruptions (Johnston, 1997), several measurements, on ground (Hayakawa, 2000; Gokhberg, 1979) and by experiments on low-Earth orbit satellites (e.g. IKB-1300, Intercosmos-19 and 24, COSMOS 1809, Aureol-3, Gamma-1, Maria-2, Electron, SAMPEX, NOAA, Demeter, etc. De Santis (2015) and the references therein) revealed: electromagnetic and plasma perturbations and anomalous increases of high-energy particle flux (De Santis, 2015). The precipitation of trapped electrons and protons (from a few MeV to several tens of MeV) from the inner radiation belts could be induced by pitch-angle diffusion (Aleshina et al., 1992) due to seismo-electromagnetic emissions before (a few hours) earthquakes (Sgrigna, 2005). Due to the longitudinal drift along a same L-shell, anomalous particle bursts could be detected by satellites not only on the epicentral area of the incoming earthquake, whereas the opposite drift directions of positive and negative particles could allow reconstructing the longitude of the earthquake focal area (Alexandrin, 2003). The claims that the reported anomalies are seismic precursors (Molchanov and Hayakawa, 1993, 1994; Molchanov et al., 1995) are still intensely debated (Rodger, 1999), but the lithosphere-atmosphere-ionosphere coupling (LAIC) mechanism, suggested by Pulinets and Boyarchuk (2005), could be able to explain some aspects of the phenomenology. Any way, data and analyses for testing claimed correlations are still lacking. In fact, ionospheric currents, plasma parameters and stability of Van Allen belt are constantly modified by natural non-seismic and man-made processes. An important role in controlling the dynamic of the topside ionosphere is played by the Sun that generates (regular and irregular) variations of the ionosphere-magnetosphere parameters as well as by the tropospheric activity. In order to identify seismo-associated perturbations, it is needed to reject the “normal” background effects of the e.m. emissions due to: lightning (whistlers), geomagnetic storms and artificial emitters (e.g. power lines, VLF transmitters, HF stations, etc.).

Many analyses have shown that satellite observations of electromagnetic fields, plasma parameters and particle fluxes in low Earth orbit may be useful in order to study the existence of electromagnetic emissions associated with seismicity (Parrot, 1993). Although the earthquakes forecasting is not possible today (Sgrigna, 2007), it is certainly a major challenge – and perhaps even a duty – for science in the near future. Currently, the only available large database is that collected by the Demeter satellite (Parrot, 2002) and by rare observations made by some previous space missions, non-dedicated to this purpose. The CSES satellite aims at continuing the exploration started by Demeter (Lagoutte, 2006) with advanced multi-parametric measurements of energetic particle fluxes, ionospheric plasma parameters and electromagnetic fields, in a wide range of energy and frequencies. In this framework, CSES mission can also investigate the structure and the dynamic of the topside ionosphere, the coupling mechanisms with the lower and higher plasma layers and the temporal variations of the geomagnetic field, in quiet and disturbed conditions.

The second main objective of the mission is to study solar-terrestrial interactions and phenomena of solar physics. The flux of galactic cosmic rays is significantly modified by the solar cycle that affects the original differential spectra. The resulting solar modulation effect is evident in neutron monitor data, showing a clear anti-correlation between particle intensities and solar activity (Mathews, 1971). Particles with rigidities up to at least 30 GV are mainly affected and the effect becomes progressively larger as the rigidity decreases (Iskra, 2015). Moreover, solar activity is characterized by a number of transient phenomena such as solar flares, Coronal Mass Ejections, etc. The ejected particles can be accelerated at energies ranging from a few tens of KeV up to a few GeV (Solar energetic particles – SEP) (Verkhoglyadova, 2015), can escape the Sun magnetic field and reach the Earth causing geomagnetic disturbances, magnetic storms, etc. CSES mission will be able monitor both the solar impulsive activity and cosmic ray solar modulation, by detecting proton and electron fluxes from a few MeV up to hundreds of MeV. The measurements will provide an extension up to very low energy of the range of the particle spectra that are currently monitored (at higher energy) by PAMELA (Picozza, 2007) and AMS (Aguilar, 2013) experiments. It will be also

Table 1
HEPD main technical characteristics.

Free field of view:	≥70°	Orientation:	Zenith
Mass budget:	<35 Kg	Power budget:	≤38 W
Dimensions:	20 × 20 × 40 cm^3	Operative temp.:	−10° ± 45°
Operating modes:	Survey and Burst	Lifetime:	≥5 years

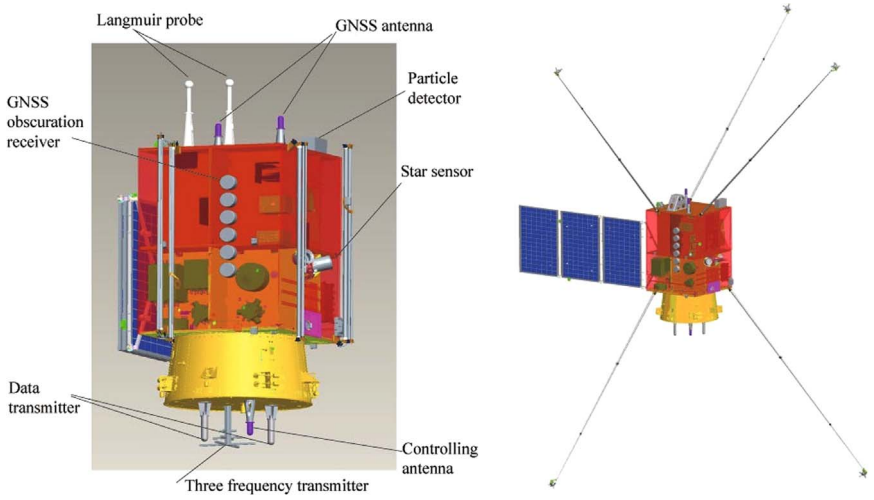

Fig. 1. CSES satellite before and after the deployment of the solar panels and of the 4 booms where are installed the probes of the electric field detector (EFD). It is possible to see also the HEPD (installed on the top, pointing to Zenith) and some of the other on board instruments.

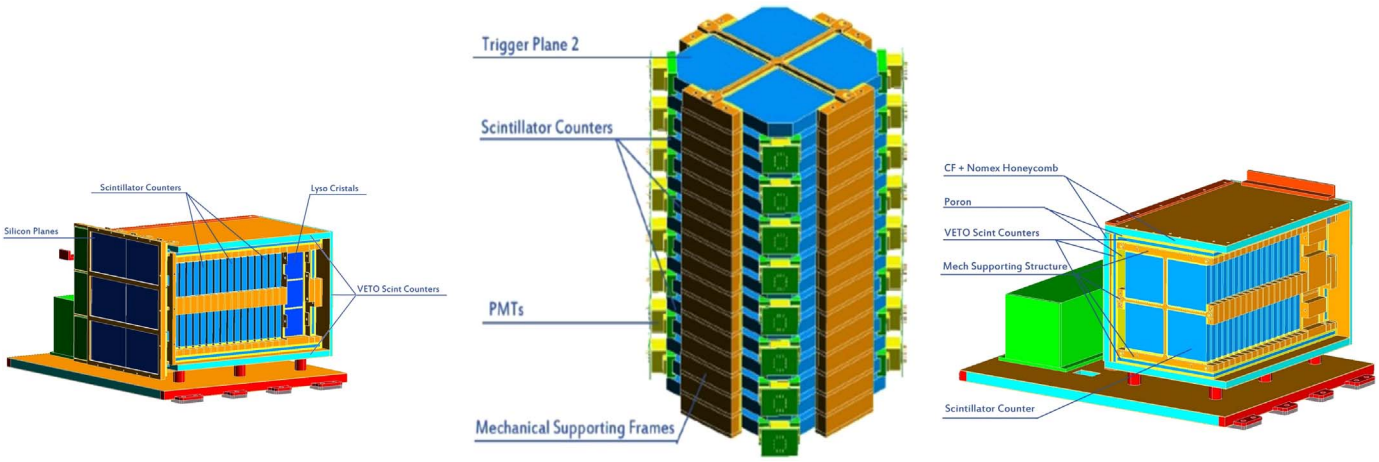

Fig. 2. Several views of the layout of the HEPD instrument. From left to right: longitudinal view of the detector with the silicon tracker (in blue) on the top of the scintillator counters (vertical layers coloured in cyan); tower of scintillators with PMTs (panel in the middle); detailed view of the detector with the veto counters (in light blue) and the mechanical support. (For interpretation of the references to color in this figure, the reader is referred to the web version of this article.)

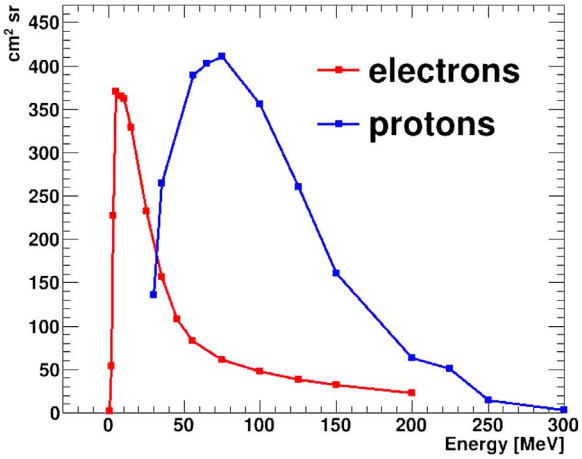

Fig. 3. Energy acceptance for protons and electrons that can be detected by HEPD.

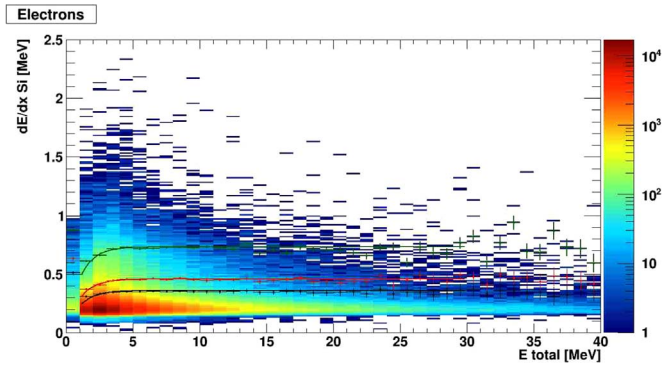

Fig. 5. Selection cuts in the electron sample with efficiencies at 90% (black), 95% (red) and 99% (green). (For interpretation of the references to color in this figure, the reader is referred to the web version of this article.)

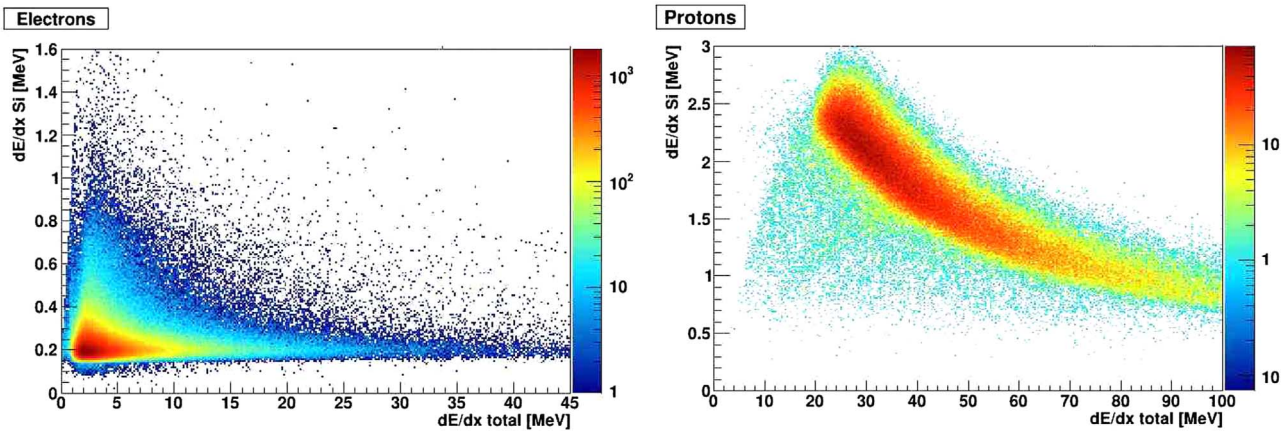

Fig. 4. Distributions of the energy loss in the silicon tracker and in the whole detector for electrons and protons.

possible to compare the spectra measured by CSES with those from other space mission, such as GOES (Davis, 2007) and ACE (Maruyama and Takashi, 1997).

2. The CSES satellite and the LIMADOU collaboration

Seismic precursors have been investigated in space by the Demeter satellite (Lagoutte, 2006) and some other projects have been conceived (e.g. Esperia, Vulkan, Quakefinder, Lazio-Egle, Arina, etc.). In this framework, on 2013, the Chinese (CNSA) and the Italian (ASI) space agencies signed an agreement to develop the China Seismo-Electromagnetic Satellite (CSES) that aims at investigating electromagnetic field, plasma and particles in the near-Earth environment in order to study in particular seismic precursors, particles fluxes (from Van Allen belts, cosmic rays, solar wind, etc.), anthropogenic electromagnetic pollution and more in general the atmosphere-ionosphere-

Fig. 6. Picture of the HEPD flight model (FM): assembly (left) and at the thermal-vacuum acceptance test (right).

Table 2
Main characteristics of the EFD instrument.

Frequency range	ADC bits	Sampling data rate	Dynamic range (dB)		Output
			Analog chain	ADC	
~0–16 Hz	31	1 Ksps	120	124	Waveform
13 Hz–2 kHz	24	1 Msps	139	105	Waveform
1–50 kHz	24	1 Msps	115	105	Spectrum
21 kHz–5 MHz	16	128 Msps	87	78	Spectrum

magnetosphere coupling mechanisms that can affect the climate changes. The launch of CSES - the first of a series of several satellite missions - is scheduled by the Summer of 2017 on a Sun-synchronous orbit: 97.4°, 507 km, for a lifetime ≥5 years. The CSES satellite has been financed by the CNSA (China National Space Agency) and developed by CEA (China Earthquake Administration) together with several Chinese research institutes and private companies such as the DFH (that has developed the CAST2000 satellite platform). The Italian participation to the CSES mission, called LIMADOU-collaboration, includes the Universities of Roma Tor Vergata, Uninettuno, Trento, Bologna and Perugia, as well as the INFN (Italian National Institute of Nuclear Physics), INGV (Italian National Institute of Geophysics and Volcanology) and INAF-IAPS (Italian National Institute of Astrophysics and Planetology). The sensors onboard the satellite are SitoCses (): the HEPD (High Energy Particle Detector); a low energy particle detector (HEPP); two Langmuir Probes; a plasma analyser that includes an ion capture meter ICM) and a retarding potential analyser (RPA); the EFD (Electric Field Detector); a high precision magnetometer (HPM); a search-coil magnetometer (SCM); a GNSS Occultation Receiver and a Tri-Band Beacon transmitter. The LIMADOU collaboration has built the High Energy Particle Detector (HEPD); has participated to develop the Electric Field Detector (EFD) and is performing several test campaign of the Langmuir probes and of the plasma analyser in the INAF-IAPS Plasma Chamber (PlasmaChamb) in Rome. In this facility the response of the sensors, and their compatibility with ionospheric plasma, can be verified in environmental conditions very similar to those met by the satellite in orbit.

3. The High Energy Particle Detector (HEPD)

The LIMADOU collaboration has projected and built the HEPD instrument on the basis of a long experience in developing advanced space detectors for charged and neutral particles and gamma rays – in a wide range of energies – for applications in solar physics as well as in extragalactic astrophysics and cosmology. The previous detectors, devoted to study cosmic rays, anti-matter, dark matter, etc. have been adopted in many missions on balloons (MASS, CAPRICE, etc. Papini (2004)), small satellites (NINA, NINA-2, etc.), inside the International Space Station (SilEye, ALTEA, etc) and finally in the large PAMELA satellite mission (Wizard; Adriani, 2016) Fig. 1.

HEPD, installed on the top of CSES spacecraft, pointing to zenith, can identify electrons (3–200 MeV), protons (30–300 MeV) and light nuclei up to iron, with high energy and high angular resolutions needed to reconstruct the particles pitch angle. The main characteristics of the instrument are summarized in Table 1. Due to the CSES high inclination orbit, HEPD can detect particles of different nature that will complement PAMELA data at lower energy. HEPD consists of a tower of 16 layers of plastic scintillator ($15 \times 15 \times 1$ cm^3) and a 3×3 matrix of LYSO (for a resulting plane of dimension $15 \times 15 \times 4$ cm^3), read out by PMTs (Fig. 2). The direction of particles is provided by 2

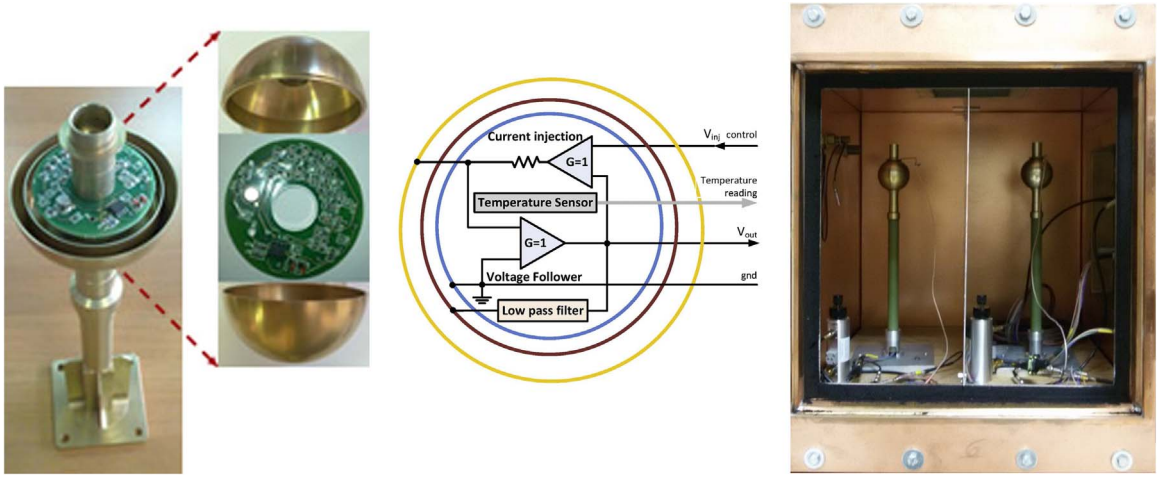

Fig. 7. From left to right: exploded view of one EFD probe with the internal electronic board; block-diagram of the sensor; photo of two EFD sensors installed in the Faraday cage during the test campaign. In order to reduce the asymmetry introduced by the presence of the boom, a short stub is installed on each probe of the EFD (on the other side with respect the boom axis) and is bootstrapped at the same potential of the sensor.

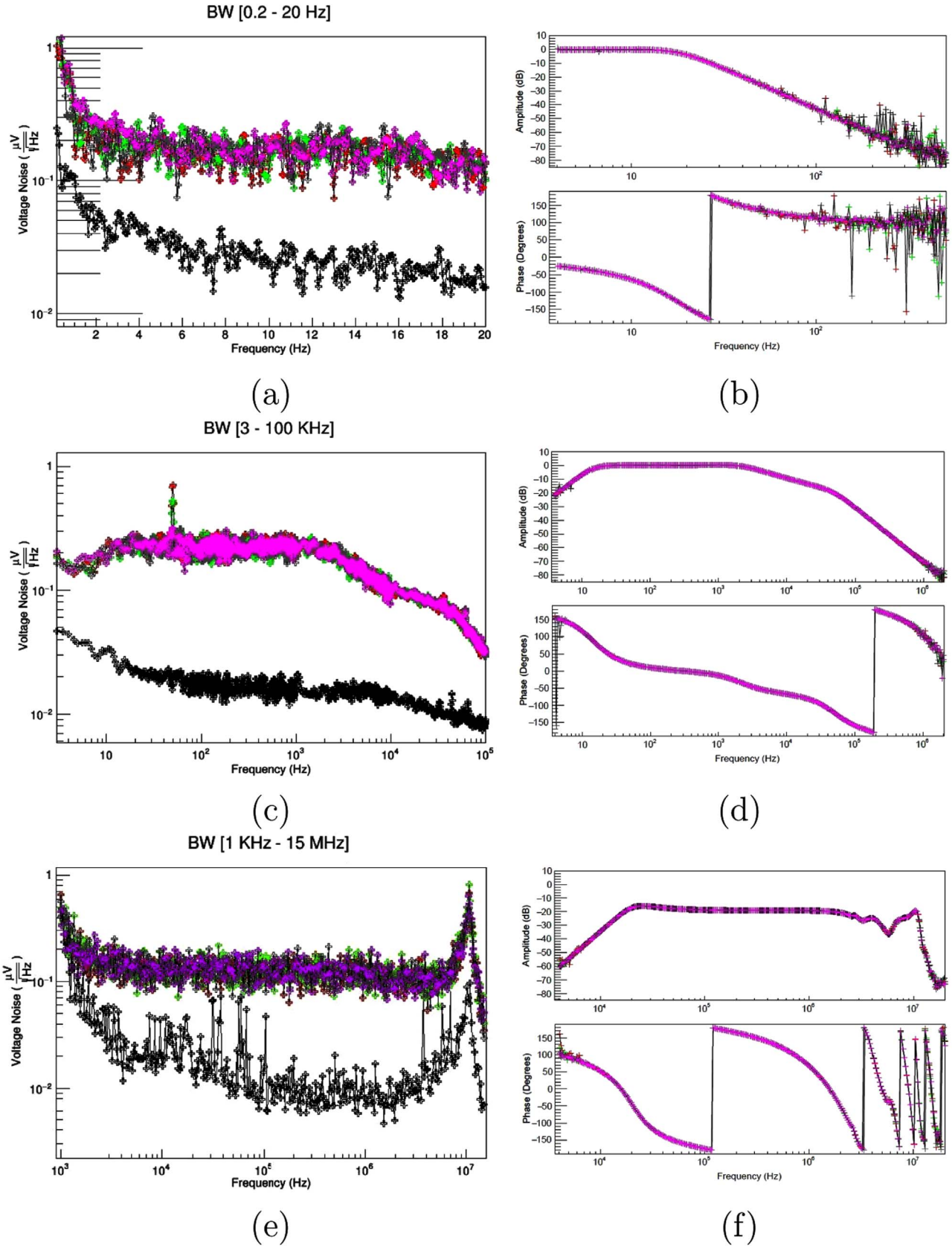

Fig. 8. Voltage noise spectral density vs frequency (panels a,c, and e) and EFD transfer function (panels b,d, and f) for low, medium and high frequency ranges (panels from top to bottom). Measurements have been executed with an equivalent electric circuit (with impedance of $R = 660\ \mathrm{k}\Omega$ and $C = 6.6\ \mathrm{pF}$) which represents the plasma coupling impedance for medium plasma condition (i.e. medium values of electron temperature and density), and for several values of the injected bias current, necessary to optimize the coupling with the plasma along the orbit. The black traces represent the noise due to only the measurement instrumentation, while the EFD electronics is powered off (background); red, green, grey and violet traces have been obtained with bias currents of 0 nA, 100 nA, −150 nA and −300 nA respectively. (For interpretation of the references to color in this figure, the reader is referred to the web version of this article.)

planes of double-side silicon microstrip at the top of the detector in order to limit the Coulomb multiple scattering. Veto planes (5 mm thick) of plastic scintillator surround the detector. Electron angular resolution is 13° at 2.5 MeV and ≤1° above 35 MeV; angular acceptance >60° at (2.5 – 100) MeV; angle-integrated total acceptance >100 cm^2 sr at (2.5 – 35) MeV and ~40 cm^2 sr at 100 MeV. Protons angular resolution is ≤1° over the full detection range; integrated-angle total acceptance >100 cm^2 sr at (30 – 150) MeV and 60 cm^2 sr at 200 MeV. HEPD performances have been estimated via a Geant4 simulation of $5{\cdot}10^6$ particles at fixed energy bins (in the range (1 – 200) MeV for electrons and (30 – 500) MeV for protons) and hundred million particles with a power law spectrum. Particles were generated with $0° \le \theta < 90°$ where θ is the angle between the direction of the incoming particle and the longitudinal axis of the detector. The angle-integrated electron and proton acceptances are presented in Fig. 3. Because in the HEPD energy range protons are slow and not relativistic, the e^-/p^+ discrimination is evaluated by the ratio between the energy deposited in the 2 silicon trackers and that released in the whole detector. The resulting 2-dimensional distributions for electrons and protons, shown in Fig. 4, are very different and particles lay in separate energy bands. HEPD allows identifying electrons with acceptable proton background levels (10^{-5} – 10^{-3}). The proton contamination in the electron sample has been estimated by applying different cuts with efficiencies of 90%, 95% and 99% in the electron selection (see the three curves adopted in Fig. 5). In order to assess the compliance of HEPD to the operation requirements in space and to execute the detector calibration, several test and qualification campaigns were performed on the Qualification Model (QM) and the Flight Model (FM) (see Fig. 6). The space qualification measurements – executed at SERMS laboratory in Terni (IT) – included thermo-vacuum and vibration tests. In order to study the instrument response to charged particles: the QM has been tested at the Beam Test Facility (BTF) of the LNF-INFN laboratories, with electrons and positrons of 30–150 MeV; the FM has been tested both at BTF (with electrons and positrons of 30–120 MeV), and at the "Centro di Protonterapia" of APSS in Trento (with proton of 37–225 MeV). Both QM and FM were operated via the Electrical Ground Support Equipment (EGSE) device, which simulates the satellite interfaces. Further studies were carried out by means of the acquisition of cosmic-ray muons.

4. The electric field detector (EFD)

The EFD is an advanced detector for space-based measurements of electric field in a wide frequency band, specifically conceived for operation in the ionosphere-magnetosphere transition zone. The instrument, designed to be installed on the 3-axes stabilized CSES satellite, includes: 4, probes exposed to the ionospheric plasma, accommodated on the tip of 4 booms (each of them four meters long, deployed far from the spacecraft body in order to reduce the electromagnetic disturbances induced by the satellite equipment), and a data acquisition unit (for signal conditioning, sampling of input signals and spectral analysis). EFD retrieves the electric field components from the d.o.p. measured between pairs of probes, in the bands: ~ DC – 16 Hz; 13 Hz - 2 kHz; 1 – 50 kHz and 21 kHz – 5 MHz. The main characteristics of the instrument are summarized in Table 2. The voltage of an electrode in plasma is a function of the collected current that is function of the current/voltage characteristic. Because a floating electrode in plasma, usually, acquires a negative potential, a current generator is needed to bias EFD close to the plasma potential in order to minimize the contact impedance and to improve the measurement accuracy. Fig. 7 shows the photos and the block diagram of one EFD sensor. The performance of the EFD instrument have been tested in a Faraday cage, in order to shield the probes from the external electromagnetic interferences, and in the plasma chamber of the INAF-IAPS (PlasmaChamb) that allows simulating the typical plasma conditions along the satellite orbit. The test campaign has been carried out by varying both the equivalent electric circuit (which represents the plasma coupling impedance) and the bias current. We have estimated the values of the plasma impedance for 3 different combinations of plasma densities and temperatures (Badoni, 2015), which can be considered as the typical extreme values and the medium value expected along the orbit of a LEO satellite such as CSES. Fig. 8 shows the voltage noise spectral densities and the transfer function for the low, medium and high frequency channels, measured in medium electron temperature/density plasma conditions ($T \sim 2000$ K, $\rho \sim 10^{10} m^{-3}$).

5. Conclusions

CSES satellite will study the near Earth electromagnetic, particle, and plasma environment with aim at: (i) investigating precipitation of particles and electromagnetic fluctuations possibly induced by earthquakes and (ii) solar-terrestrial interactions with special focus on solar energetic particle emissions and modulation of cosmic rays (Boezio, 2000, 1999). The LIMADOU collaboration has built the HEPD detector of charged particles and the electric field detector EFD. The qualification and the flight models of the HEPD have been fully tested in laboratory and at several beam test facilities; the flight model will be shipped by the and of 2016. The EFD has been built and fully tested at the INAF-IAPS's plasma chamber in Rome, Italy. In the CSES configuration (with a distance of about 8 m between each pair of probes), EFD achieves: a resolution in the ULF band better than ~1 μ V/m (40 times better than the most recent instruments of similar features (such as for example the ICE detector of the DEMETER mission (Berthelier, 2006)), and in the other bands a sensitivity of the electric field better than 50 nV/($\sqrt{Hz}$ m). The launch of the CSES satellite is scheduled for July–August 2017.

References

Adriani, O., et al., 2016. Astrophys. J. - ApJ 818 (1), 68.
Aguilar, M., et al., 2013. Phys. Rev. Lett. 110.14, 141102.
Aleshina, M.E., Voronov, S.A., Galper, A.M., et al., 1992. Cosm. Res. 30 (1), 79.
Alexandrin, S.Y., et al., 2003. Ann. Geophys. 21, 597.
Badoni, D., et al., 2016. In: Proceedings 34th ICRC 2015,The Hague, The Netherlands, July 30-August 6, PoS, 2016, 588, SISSA (2015-08-01).
Berthelier, J.J., et al., 2006. Planet Space Sci. 54, 456–471.
Boezio, M., et al., 1999. Astrophys. J. 518, 457.
Boezio, M., et al., 2000. ApJ 532, 653.
Davis, G., 2007. Journal of Applied Remote Sensing 1.1: 012504–012504.
De Santis A., et al., 2015. Physics and Chemistry of the Earth Parts A/B/C, http://dx.doi.org/10.1016/j.pce.2015.05.004
Gokhberg, M.B., et al., 1979. Dokl. Acad. Sci. USSR 248, 1077–1081.
Hayakawa, et al., 2000. Phys. Chem. Earth A 25, 263–269.
Iskra, K., et al., 2015. Journal of Physics: Conference Series. Vol. 632. No. 1. IOP Publishing, 2015.
Johnston, M.J.S., 1997. Surv. Geophys. 18, 441–475.
Lagoutte, et al., 2006. Planet. Space Sci. 54, 428–440.
Maruyama, Takashi, et al., 1997. Review of the Communications Research Laboratory, vol. 43, p. 285 43: 285.
Mathews, T., et al., 1971. Nature (22 January); 229, 246–247 http://dx.doi.org/10.1038/229246a0
Molchanov, O.A., Hayakawa, M., et al., 1993. Ann. Geophys. 11, 431–440.
Molchanov, O.A., Hayakawa, M., 1994. Ed. Hayakawa, M. (TERRAPUB), p. 537–563.
Molchanov, O.A., Hayakawa, M., Rafalsky, V.A., 1995. J. Geophys. Res. 100, 1691–1712.
Papini, P., 2004. Astrophys. J. 615, 259.
Parrot, M., 2002. J. Geodyn. 33, 535–541.
Parrot, M., et al., 1993. Phys. Earth Planet. Inter. 77, 65–83.
Picozza, P., et al., 2007. Astropart. Phys. 27.4, 296–315.
⟨http://www.iaps.inaf.it/downloads/2016-INAF-IAPS-PlasmaChamb⟩
Pulinets, S., Boyarchuk, K., 2005, ISBN: 978-3-540-20839-6.
Rodger, C.J., et al., 1999. In: Atmospheric and Ionospheric Electromagnetic Phenomena Associated with Earthquakes, edited by M. Hayakawa, pp. 697–710, TERRAPUB, Tokyo.
Sgrigna, V., et al., 2005. J. Atmos. Solar-Terr. Phys. 67, 1448–1462.
Sgrigna, V., et al., 2007. Tectonophysics 431, 153–171.
⟨http://cses.roma2.infn.it/instruments⟩
Verkhoglyadova, O.P., et al., 2015. Phys. Rep. 557, 1–23.
⟨http://wizard.roma2.infn.it/⟩
Xuhui, S., et al., 2011. Earthq. Sci. 24 (December (6)), 639–650.